Hydrogen Productions Hot Paper

International Edition: DOI: 10.1002/anie.201606972
German Edition: DOI: 10.1002/ange.201606972

Achieving High Efficiency and Eliminating Degradation in Solid Oxide Electrochemical Cells Using High Oxygen-Capacity Perovskite

*Areum Jun, Junyoung Kim, Jeeyoung Shin, and Guntae Kim**

Abstract: *Recently, there have been efforts to use clean and renewable energy because of finite fossil fuels and environmental problems. Owing to the site-specific and weather-dependent characteristics of the renewable energy supply, solid oxide electrolysis cells (SOECs) have received considerable attention to store energy as hydrogen. Conventional SOECs use Ni-YSZ (yttria-stabilized zirconia) and LSM (strontium-doped lanthanum manganites)-YSZ as electrodes. These electrodes, however, suffer from redox-instability and coarsening of the Ni electrode along with delamination of the LSM electrode during steam electrolysis. In this study, we successfully design and fabricate highly efficient SOECs using layered perovskites,* $PrBaMn_2O_{5+\delta}$ *(PBM) and* $PrBa_{0.5}Sr_{0.5}Co_{1.5}Fe_{0.5}O_{5+\delta}$ *(PBSCF50), as both electrodes for the first time. The SOEC with layered perovskites as both-side electrodes shows outstanding performance, reversible cycling, and remarkable stability over 600 hours.*

In recent years, there have been increasing demands for clean and renewable energy sources owing to heavy dependence on fossil fuels and environmental problems.[1,2] However, the supply of renewable energy struggles to match demands because it is weather-dependent and site-specific. Therefore, these problems have motivated researchers to develop energy storage devices such as secondary batteries, ultracapacitors, and water electrolyzers. But, secondary batteries and ultracapacitors have drawbacks including limited energy storage capacity, cost ineffectiveness, and loss of charge over time.[3] In this regard, water electrolysis can be a leading technology for large-scale and highly efficient energy storage. Most of the work in electrolysis has focused on low-temperature proton exchange membranes (PEM) and alkaline electrolysis cells.[4] At present, high-temperature solid oxide electrolysis cells (SOECs) have received great attention as a promising energy storage device. Compared to low-temperature alkaline and PEM electrolysis cells, SOECs have shown higher hydrogen production efficiency because electrolysis at elevated temperatures is advantageous to both the thermodynamics and kinetics of the reaction.[5] The electrical energy demand decreases considerably as the operating temperature rises owing to the increase in provided thermal energy. In addition, a high operating temperature is favorable for the faster kinetics, resulting in improved hydrogen production efficiency for the SOEC.[1]

SOECs and solid oxide fuel cells (SOFCs), which are referred to as solid oxide cells (SOCs), can operate reversibly as shown in Figure 1. The electrical energy is converted to H_2 in electrolysis mode (green line) and the electricity is produced from H_2 through fuel cell mode (orange line).[5,6] In SOECs, H_2 is produced by electrolysis of steam at the fuel electrode, and then oxygen anions (O^{2-}) diffuse through the electrolyte toward the air electrode. These anions are oxidized to oxygen to complete the reaction. The reactions in the fuel and the air electrode are:[7]

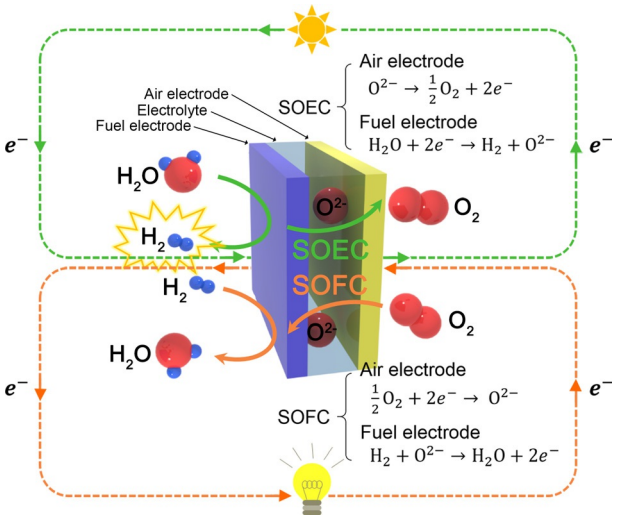

Figure 1. Illustration of a SOC system.

$$\text{Fuel electrode}: \quad H_2O + 2e^- \rightarrow H_2(g) + O^{2-} \tag{1}$$

$$\text{Air electrode}: \quad O^{2-} \rightarrow \frac{1}{2}O_2(g) + 2e^- \tag{2}$$

Generally, state-of-the-art SOECs use Ni-YSZ (yttria-stabilized zirconia) and LSM (strontium-doped lanthanum manganites)-YSZ as electrodes.[8] However, these electrodes suffer from several important limitations, such as the redox-instability and coarsening of Ni and the delamination and insufficient electrolytic performance of LSM during steam electrolysis.[9–11] LSM exhibits apparent oxygen excess non-

[*] A. Jun, J. Kim, Prof. G. Kim
Department of Energy Engineering
Ulsan National Institute of Science and Technology (UNIST)
Ulsan 44919 (Republic of Korea)
E-mail: gtkim@unist.ac.kr
J. Shin
Department of Mechanical Engineering
Dong-Eui University
Busan 47340 (Republic of Korea)

Supporting information for this article can be found under: http://dx.doi.org/10.1002/anie.201606972.

stoichiometry in an oxidation environment. This excess oxygen in LSM gives rise to the formation of cation vacancies, which is thermodynamically unfavorable in the $LaMnO_3$ perovskite structure.[12,13] The cation vacancies would cause the disintegration of LSM and the formation of cation oxides or LSM nanoparticles. It results in degradation and delamination due to severe microstructural damage near the air electrode/electrolyte interface.[14,15]

Recently, one group found that reversible cycling between electrolysis and fuel-cell modes can eliminate severe electrolysis-induced degradation. Reversible cycling with time periods of 1 hour in electrolysis mode and 5 hours in fuel-cell mode reduce the internal oxygen pressure at the air electrode/electrolyte interface during electrolysis operation, which would reduce delamination and microstructural damage.[16] But, for continuous hydrogen production, reversible cycling is not an optimal solution for electrolysis because the SOEC must be switched to SOFC.

Accordingly, it is of great significance to develop fuel and air electrode materials that can provide more active and stable performance. In recent years, many researchers have focused on layered perovskites as electrode materials for SOFCs owing to their fast oxygen kinetics and stability.[17,18] A site-layered perovskite $PrBaMn_2O_{5+\delta}$ (PBM) exhibited high and durable performance and excellent redox stability.[6] Also, a layered $PrBa_{0.5}Sr_{0.5}Co_{1.5}Fe_{0.5}O_{5+\delta}$ (PBSCF50) perovskite was reported to provide excellent electrochemical performance and stability.[19] Furthermore, PBSCF50, in contrast to the LSM electrode, can accommodate more oxygen as oxygen interstitials, which can solve some of the problems associated with LSM.

In this study, we successfully fabricated and demonstrated the SOEC with layered perovskites as both-side electrodes for the first time. This SOEC shows high durability and performance without any coarsening and delamination of electrodes for a long time.

The phase reaction between the electrode and electrolyte can generate an undesired insulating layer at the interface, which obstructs the oxide-ionic and electronic transport.[20] Therefore, it is essential to avoid any insulating phases during electrochemical reaction for the reliable operation of the SOEC. The chemical reactivity of each electrode with LSGM electrolyte was evaluated by analyzing the X-ray diffraction (XRD) patterns. Figure 2a and b show XRD patterns of the PBSCF50-GDC/LSGM and PBM(Co-Fe)/LDC/LSGM. There are no observed interfacial reactions or undesirable secondary phases between each electrode and LSGM.

The microstructure of the pristine SOEC is shown in Figure 2c and d. Figure 2c presents a cross section of PBSCF50-GDC/LGSM, and Figure 2d shows a cross section of PBM(Co-Fe)/LDC/LSGM. The cell has ≈20 μm porous electrodes and a ≈5 μm LDC buffer layer, which prevents any inter-diffusion of ionic species between the PBM and LSGM. The interface between the electrode/buffer layer and the electrolyte appears to be well-connected without any delamination.

Figure 3a shows the *I–V* curves in this study at different temperatures. H_2 gas containing 10% steam was fed to the fuel electrode and the air electrode was exposed to an air.

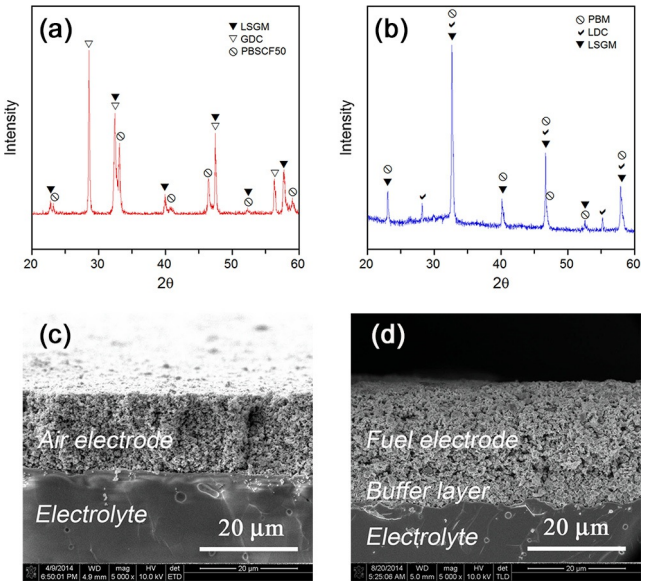

Figure 2. XRD patterns of a) PBSCF50-GDC/LSGM and b) PBM (Co-Fe)/LDC/LSGM. SEM images of c) PBSCF50-GDC/LSGM and d) PBM (Co-Fe)/LDC/LSGM interfaces of the single cell before electrolysis tests.

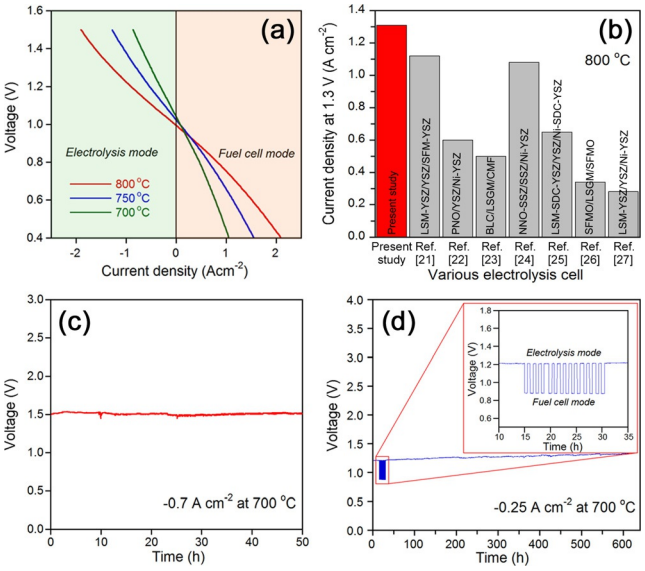

Figure 3. a) *I–V* curves for the single cell measured at various temperatures. b) Comparison of the current density at 1.3 V and 800 °C of the present work and other literature studies. c) The short-term stability of the single cell under $-0.7\ A\,cm^{-2}$ at 700 °C. d) The long-term stability and reversible cycling test for $-0.25\ A\,cm^{-2}$ at 700 °C. The inset shows the reversible cycling result that was performed at $-0.25\ A\,cm^{-2}$ (electrolysis mode) and at $+0.25\ A\,cm^{-2}$ (fuel cell mode).

Current densities of 1.31, 0.81, and 0.52 $A\,cm^{-2}$ were obtained at 800, 750, and 700 °C, respectively, at 1.3 V close to the thermoneutral voltage. At thermoneutral voltage, which is around 1.29 V for steam electrolysis, the electricity input into the cell and the total energy demand for electrolysis reaction are equal. Therefore, the electricity-to-hydrogen conversion efficiency is 100% at this voltage.[8,16] A Nyquist plot of the

impedance data measured at OCV in electrolysis mode is presented in Figure S1. The non-ohmic resistance was determined by the impedance intercept between the high and low frequency intercepts, including charge and non-charge transfer processes for the electrode electrolysis reaction,[20] which decreased with increasing temperature: 0.074, 0.118, and 0.161 $\Omega\,cm^2$ at 800, 750, and 700 °C, respectively.

Figure 3b and Table S1 show the electrolysis performance data of this work and other reports.[21–27] The performance of the present work (1.31 $A\,cm^{-2}$) is higher than that of the nanostructured $Sr_2Fe_{1.5}Mo_{0.5}O_{6-\delta}$-YSZ and LSM-YSZ electrode based single cell (1.12 $A\,cm^{-2}$) under the same steam feeding condition.[21] This result is also more than 10-fold better than that of prior report for perovskite LSM and $La_{0.4}Sr_{0.4}Ni_{0.06}Ti_{0.94}O_{2.94}$ electrode (0.13 $A\,cm^{-2}$ at 900 °C) even with lower operating temperature.[28] Moreover, this work is superior to that reported in the literature for Ni-YSZ supported cell with LSM-YSZ composite air electrodes (1.0 $A\,cm^{-2}$ at 850 °C).[29]

Electrolysis operating conditions give higher $p(O_2)$ to the interface between air electrode and electrolyte (that is, >0.21 atm) due to oxygen evolution [Eq. (2)]. Figure S2 shows the oxygen nonstoichiometry of the PBSCF50 and LSM as a function of $p(O_2)$ at 700 °C. At 0.21 atm, PBSCF50 shows oxygen-deficient nonstoichiometry while LSM shows oxygen-excess nonstoichiometry. Excess oxygen in LSM can form cation vacancies because oxygen ions do not participate in the interstitial position of the close-packed ABO_3 type perovskite structure owing to their larger ionic radii. From a neutron diffraction study, Tofield and Scott reported the existence of cation vacancies at both La and Mn sites.[15,30] Thus, it is assumed that metal vacancies on both La and Mn are the predominant defects in the higher $p(O_2)$ region. In the oxygen excess region, the formation of cation vacancies in LSM may be expressed as:

$$6Mn_{Mn}^{X} + \frac{3}{2}O_2 \leftrightarrow V_{La}^{'''} + V_{Mn}^{'''} + 3O_O^X + 6Mn_{Mn}^{\bullet} \quad (3)$$

Therefore, the cation vacancies would cause disintegration of LSM and the formation of cation oxide or LSM nanoparticles, resulting in severe microstructural damage near the air electrode/electrolyte interface, eventually, leading to degradation and delamination.[31] However, the layered perovskite, PBSCF50, can accommodate excess oxygen as the form of oxygen interstitials within the Pr–O plane in the electrolysis region, thereby effectively inhibiting the creation of any cation vacancies.[19] This would exclude some drawbacks of the LSM electrode,[32] and lead to improved stability in the electrolysis mode.

Operating the electrodes under high current densities results in an increased H_2 production rate and more efficient usage of the surplus electricity. In the LSM-YSZ/YSZ/Ni-YSZ cell operated at high current densities, anodic polarization of the LSM-YSZ air electrode increases $p(O_2)$ at the air electrode/electrolyte interface, resulting in accelerated degradation along with delamination.[11] To assess the stability of the single cell at high current density, the voltage of the cell was recorded under a constant high current of $-0.7\,A\,cm^{-2}$ at 700 °C (Figure 3c). The voltage of this cell was almost constant with no degradation at $-0.7\,A\,cm^{-2}$ for 50 hours, demonstrating that the PBM(Co-Fe)/LDC/LSGM/PBSCF50-GDC cell can operate at high current densities and produce more H_2 than the Ni-YSZ/YSZ/LSM-YSZ cell.

Ideally, SOECs can operate in a reversible mode as a SOFC; that is, reversible SOCs produce H_2 from steam (electrolysis) and subsequently use the produced H_2 to generate electrical energy (fuel cell).[8] However, the SOEC is significantly different from the SOFC when considering the fuel electrode reaction under high humidity conditions. Figure 3d shows the reversibility and long-term stability of the SOEC at 700 °C under 10 % steam and 90 % H_2 fed in the fuel electrode side. Over 15–30 hours, the reversibility of operation (Figure 3d, inset) was confirmed by cycling between electrolysis at $-0.25\,A\,cm^{-2}$ and fuel cell operation at $+0.25\,A\,cm^{-2}$. The cell shows stable performance in both electrolysis and fuel cell mode without noticeable degradation during 14 cycles. After reversible cycling, the voltage remained almost constant without observable degradation for over 600 hours at $-0.25\,A\,cm^{-2}$. It is speculated that the better redox stability, high mixed oxide ionic and electronic conductivity, and fast oxygen kinetics of PBM and PBSCF50 affect the high electrolysis performance and stability of the SOEC consisting of PBM and PBSCF50 as electrodes.[6,19]

To compare the microstructural stability of layered perovskite electrodes and conventional electrodes, Figure 4 shows the microstructure of conventional LSM[31] and Ni[33] electrode reported in the literature and PBSCF50 and PBM electrode before and after electrolysis stability test. As depicted in Figure 4a, the LSM electrode delaminates from the YSZ electrolyte. In Figure 4b, the Ni electrode exhibits coarsening after aging on account of its inherently poor redox

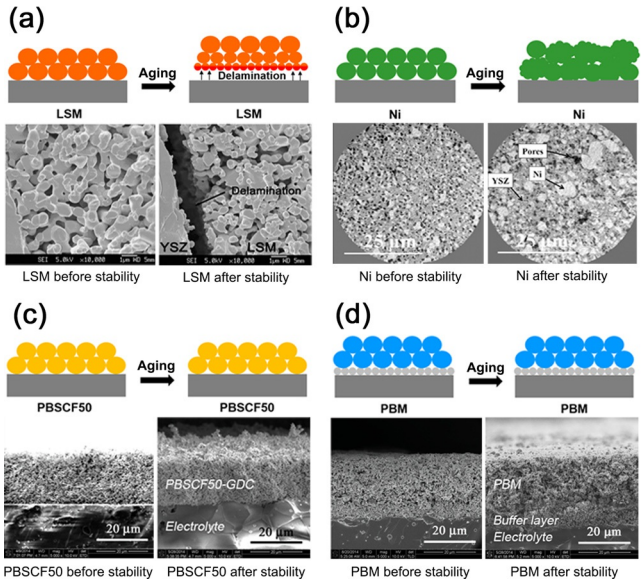

Figure 4. The SEM images and illustration of microstructural changes after an aging test of a) LSM and b) Ni-YSZ electrodes before and after stability tests in the literature, and c) the PBSCF50-GDC and d) PBM electrodes before and after stability tests for over 600 hours. a) and b) is reproduced with permission from Ref. [31] and [33].

stability. In contrast, the layered perovskites, PBM and PBSCF50, maintained fine particles with no delamination after a long-term stability test (> 600 hours; Figure 4c and d).

In this study, we reported the successful application of the layered perovskite PBM and PBSCF50 as fuel and air electrodes for the efficient and continuous production of H_2. A current density of 1.31 A cm^{-2} was obtained for the SOEC using PBM and PBSCF50 as both electrodes at 800 °C at 1.3 V. Generally, the SOEC using conventional LSM and Ni as electrodes resulted in performance loss owing to delamination of LSM and poor redox stability and coarsening of Ni. In contrast, the SOEC based on PBM and PBSCF50 electrodes shows very stable H_2 production without observable degradation for more than 600 hours. The remarkable electrolysis performance and stability demonstrate that a SOEC with a configuration of PBM/LDC/LSGM/PBSCF50 is one of the most promising electrolytic systems.

Acknowledgements

This research was supported by the Mid-career Researcher Program (NRF-2015R1A2A1A10055886 and 2016R1A2B4008514) through the National Research Foundation of Korea, funded by the Ministry of Science, ICT and Future Planning.

Keywords: electrochemistry · energy storage · hydrogen production · layered perovskites · solid oxide cells

How to cite: *Angew. Chem. Int. Ed.* **2016**, *55*, 12512–12515
Angew. Chem. **2016**, *128*, 12700–12703

[1] A. Hauch, S. D. Ebbesen, S. H. Jensen, M. Mogensen, *J. Mater. Chem.* **2008**, *18*, 2331–2340.
[2] Y. Zhu, W. Zhou, Y. Chen, Z. Shao, *Angew. Chem. Int. Ed.* **2016**, *55*, 8988–8993; *Angew. Chem.* **2016**, *128*, 9134–9139.
[3] A. Jun, Y.-W. Ju, G. Kim, *Faraday Discuss.* **2015**, *182*, 519–528.
[4] C. C. Pavel, F. Cecconi, C. Emiliani, S. Santiccioli, A. Scaffidi, S. Catanorchi, M. Comotti, *Angew. Chem. Int. Ed.* **2014**, *53*, 1378–1381; *Angew. Chem.* **2014**, *126*, 1402–1405.
[5] W. Wang, Y. Huang, S. Jung, J. M. Vohs, R. J. Gorte, *J. Electrochem. Soc.* **2006**, *153*, A2066–A2070.
[6] S. Sengodan, S. Choi, A. Jun, T. H. Shin, Y.-W. Ju, H. Y. Jeong, J. Shin, J. T. S. Irvine, G. Kim, *Nat. Mater.* **2014**, *14*, 205–209.
[7] A. Jun, J. Kim, J. Shin, G. Kim, *ChemElectroChem* **2016**, *3*, 511–530.
[8] N. Q. Minh in *Hydrogen Science and Engineering: Materials, Processes, Systems and Technology* (Ed.: D. Stolten, B. Emonts), Wiley-VCH, Weinheim, **2016**, pp. 359–390.
[9] S. Wang, H. Tsuruta, M. Asanuma, T. Ishihara, *Adv. Energy Mater.* **2015**, *5*, 1401003.
[10] V. I. Sharma, B. Yildiz, *J. Electrochem. Soc.* **2010**, *157*, B441–B448.
[11] R. Knibbe, M. L. Traulsen, A. Hauch, S. D. Ebbesen, M. Mogensen, *J. Electrochem. Soc.* **2010**, *157*, B1209–B1217.
[12] J. H. Kuo, H. U. Anderson, D. M. Sparlin, *J. Solid State Chem.* **1990**, *87*, 55–63.
[13] A. Y. Zuev, D. S. Tsvetkov, *Solid State Ionics* **2010**, *181*, 557–563.
[14] K. Chen, N. Ai, S. P. Jiang, *Int. J. Hydrogen Energy* **2012**, *37*, 10517–10525.
[15] S. Sengodan, S. Ahn, J. Shin, G. Kim, *Solid State Ionics* **2012**, *228*, 25–31.
[16] C. Graves, S. D. Ebbesen, S. H. Jensen, S. B. Simonsen, M. B. Mogensen, *Nat. Mater.* **2014**, *14*, 239–244.
[17] S. Yoo, A. Jun, Y. Ju, D. Odkhuu, J. Hyodo, H. Y. Jeong, N. Park, J. Shin, T. Ishihara, G. Kim, *Angew. Chem. Int. Ed.* **2014**, *53*, 13064–13067; *Angew. Chem.* **2014**, *126*, 13280–13283.
[18] A. Jun, S. Yoo, Y.-W. Ju, J. Hyodo, S. Choi, H. Y. Jeong, J. Shin, T. Ishihara, T. Lim, G. Kim, *J. Mater. Chem. A* **2015**, *3*, 15082–15090.
[19] S. Choi, S. Yoo, J. Kim, S. Park, A. Jun, S. Sengodan, J. Kim, J. Shin, H. Y. Jeong, Y. Choi, G. Kim, M. Liu, *Sci. Rep.* **2013**, *3*, 2426.
[20] A. Jun, J. Shin, G. Kim, *Phys. Chem. Chem. Phys.* **2013**, *15*, 19906–19912.
[21] Y. Li, P. Li, B. Hu, C. Xia, *J. Mater. Chem. A* **2016**, *4*, 9236–9243.
[22] M. A. Laguna-Bercero, H. Monzón, A. Larrea, V. M. Orera, *J. Mater. Chem. A* **2016**, *4*, 1446–1453.
[23] K. Hosoi, T. Sakai, S. Ida, T. Ishihara, *Electrochim. Acta* **2016**, *194*, 473–479.
[24] T. Chen, M. Liu, C. Yuan, Y. Zhou, X. Ye, Z. Zhan, C. Xia, S. Wang, *J. Power Sources* **2015**, *276*, 1–6.
[25] C. Yang, J. Li, J. Newkirk, V. Baish, R. Hu, Y. Chen, F. Chen, *J. Mater. Chem. A* **2015**, *3*, 15913–15919.
[26] Q. Liu, C. Yang, X. Dong, F. Chen, *Int. J. Hydrogen Energy* **2010**, *35*, 10039–10044.
[27] C. Yang, A. Coffin, F. Chen, *Int. J. Hydrogen Energy* **2010**, *35*, 3221–3226.
[28] G. Tsekouras, D. Neagu, J. T. S. Irvine, *Energy Environ. Sci.* **2013**, *6*, 256–266.
[29] A. Hauch, S. H. Jensen, S. Ramousse, M. Mogensen, *J. Electrochem. Soc.* **2006**, *153*, A1741–A1747.
[30] B. C. Tofield, W. R. Scott, *J. Solid State Chem.* **1974**, *10*, 183–194.
[31] K. Chen, S. P. Jiang, *Int. J. Hydrogen Energy* **2011**, *36*, 10541–10549.
[32] A. Orera, P. R. Slater, *Chem. Mater.* **2010**, *22*, 675–690.
[33] E. Lay-Grindler, J. Laurencin, J. Villanova, P. Cloetens, P. Bleuet, A. Mansuy, J. Mougin, G. Delette, *J. Power Sources* **2014**, *269*, 927–936.

Received: July 19, 2016
Revised: August 21, 2016
Published online: September 8, 2016

